

PACS numbers: 42.15.Dp; 42.60.Da
DOI: 10.1070/QE2006v036n02ABEH008998

Gain saturation of laser beams and production and decay of phase dislocations

A.A. Malyutin

***Abstract*. The distortion of the distribution of initially pure laser modes caused by the gain saturation is simulated numerically. It is shown that the gain saturation results in a considerable enrichment of the modal spectrum of radiation accompanied by the production and decay of phase dislocations in the far-field domain and at the output of an astigmatic $\pi/2$-mode converter.**

Keywords: *Hermite – Gaussian modes, Laguerre – Gaussian modes, gain saturation, phase dislocations.*

1. Introduction

Among many types of coherent laser beams, two substantially different groups can be distinguished. The first one includes the beams propagating in a free space by changing only the scale of their transverse size and the wave-front curvature. These beams are described by the functions that are the solutions of the same paraxial wave equation (PWE). Thus, the Hermite – Gaussian (HG) modes are the PWE solution in Cartesian coordinates, the Laguerre – Gaussian (LG) modes are the PWE solution in cylindrical coordinates, and the Ince – Gaussian (IG) modes are the PWE solution in elliptic coordinates. Each of these modes is a complete set of the orthonormal functions, which can be used as a basis in the expansion of beams of an arbitrary type. In particular, any of the HG, LG, and IG modes can be represented as a superposition of modes of another type but necessarily of the same order [1, 2]. There also exist other types of complete sets of the orthonormal functions (see, for example, [3, 4]).

The second group includes the beams that change not only their scale and wave-front curvature but also their structure during propagation in a free space. The so-called spiral beams [5] also can be assigned to this group. These beams change simultaneously their scale, the wave-front curvature, and spatial structure or orientation during propagation. As a rule, the beams of this group appear during propagation through a nonlinear medium [6 – 9] or some obstacle such as an aperture, the amplitude [10] or phase [11] screen. They can be also formed due to coherent or incoherent mixing of two or more modes of the above types. Some types of spiral beams can be obtained, for example, by the coherent mixing of the LG and HG modes.

Some of the beams of the second group attract recent attention because of the peculiarities of variations in their phase structure during their propagation, which are described in terms adopted from crystallography. For example, when the field sign changes on passing through zero (phase jump by π) in the well-known pattern of Airy rings upon the diffraction of a plane wave from a circular aperture, the term 'ring edge dislocation' is used. The boundary lines between the regions of u_{mn}^{HG} HG modes with the opposite signs of the field amplitude are called linear edge dislocations. Points with the zero amplitude on the axis of the ring u_{pl}^{LG} LG modes and the phase equal to $il\varphi$ at all other spatial points (l is the azimuthal index) are called 'screw dislocations with the topological charge l'* or 'optical vortices'.

In this paper, the main attention is given to processes of saturated gain and absorption, which favour the conversion of pure HG and LG modes (beams of the first group, according to the above classification) to the beams whose propagation and transformation is accompanied by the modifications of the phase structure that are typical for the beams assigned to the second group. This phenomenon can affect especially noticeably the conversion of high-power HG beams to the LG modes.

2. Deformations of the distribution of laser beams upon gain saturation

The gain saturation effect is related to a decrease in the inverse population of an active medium during propagation of laser radiation in it. This phenomenon is typical both for laser oscillators and amplifiers. In the model of laser pulse amplification, when compensation for the inverse population from a pump source can be neglected, the gain saturation is described by the Frantz – Nodvik equation [12]

$$\frac{Q_{\mathrm{out}}}{Q_{\mathrm{s}}} = \ln\left\{1 + G_0\left[\exp\left(\frac{Q_{\mathrm{in}}}{Q_{\mathrm{s}}}\right) - 1\right]\right\}, \qquad (1)$$

A.A. Malyutin A.M. Prokhorov General Physics Institute, Russian Academy of Sciences, ul. Vavilova 38, 119991 Moscow, Russia; e-mail: amal@kapella.gpi.ru

Received 5 May 2005; revision received 3 November 2005
Kvantovaya Elektronika **36** (2) 139 – 144 (2006)
Translated by M.N. Sapozhnikov

* The topological charge can be either positive or negative depending on the phase variation during a bypass of a singularity (where the field amplitude is zero and the field phase is not defined), either by $+2\pi l$ or $-2\pi l$.

where $Q_{in}(x, y)$ and $Q_{out}(x, y)$ are the distributions of the radiation energy density at the input and output of the amplifier (x and y are the coordinates perpendicular to the pulse propagation direction); Q_s is the saturation energy density of the active medium; and G_0 is the small-signal gain ($Q_{in} \ll Q_s$). In principle, Q_{in} is also a function of time, which, in the presence of saturation, results in the deformation of the laser pulse envelope [$Q_{out}(t)$ differs from $Q_{in}(t)$] and in a change in the radiation pattern in time; however, these effects will not be considered here in detail.

In the calculations presented below, which were performed by using the FRESNEL program [13], the calculation algorithm is based on relation (1) with the subsequent determination of the absolute value of the field in the beam and addition of the phase factor corresponding to the distribution of the initial mode field. It is considered that the amplification itself occurs in the plane coinciding with the laser beam waist, which assumes that the amplifier length is small compared to the Rayleigh length of the beam $z_R = \pi w_0^2/\lambda$ (w_0 is the beam-waist radius). The latter assumption is valid for most laser amplifiers.

2.1 Distortions of the distribution of laser beams in the near- and far-field domains

The radial mode distribution in a laser beam was analysed in model simulations directly at the amplifier output (near-field domain) and in the rear focal plane of a focusing lens (far-field domain). The amplifier was located in the front focal plane of the lens.

The distortions of two HG modes, u_{00}^{HG} and u_{10}^{HG}, were considered for quite realistic (from the practical point of view) values of the gain $G_0 = 4$ and 16 and the maximum energy density of the input beams $Q_{in}^{max} = 0.1Q_s$. The radiation from a neodymium laser was considered ($\lambda = 1055$ nm, $Q_s = 4.5$ J cm^{-2}) with the beam-waist radius $w_0 = 0.07$ cm and energy in the range between 3.5 and 7 mJ depending on the HG mode type.

The results of calculations for the u_{00}^{HG} mode presented in Figs 1a, b show that upon the gain saturation on the beam axis (where the radiation energy density is maximal), phase dislocations appear in the far-field domain at the periphery of the radiation pattern (the angular coordinate in the far-field domain is expressed in the units of divergence $\theta_{e^{-2}} = \lambda/\pi w_0$ of a Gaussian beam). The number of dislocations, which are similar in character to diffraction Airy rings, and the relative intensity of ring maxima increase with increasing the gain G_0.

For the odd mode u_{10}^{HG} (Figs 1c, d and Fig. 2), the far-field phase dislocations are of a different type. In particular, they never intersect the x axis (the index $m = 1$) for any G_0. This property is absent upon the gain saturation for other modes of type u_{m0}^{HG} with $m \neq 1$.

The gain saturation can be quantitatively characterised by the expansion of radiation at the amplifier output in the basis of the unperturbed HG modes, in which all the weight coefficients a_{jk} can be determined from the expression

$$a_{jk} = \int_{-\infty}^{+\infty}\int_{-\infty}^{+\infty} G_{nf}(u_{mn}^{HG})u_{jk}^{HG}\,dx\,dy, \qquad (2)$$

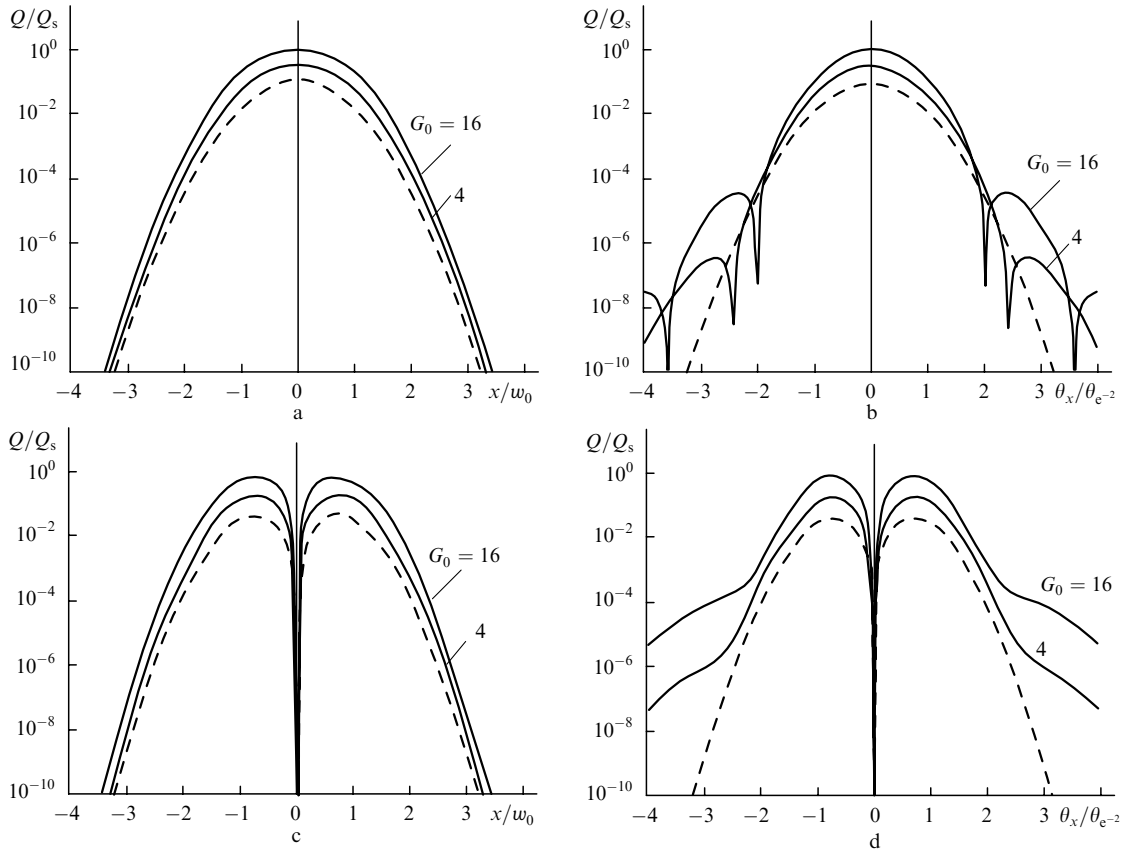

Figure 1. Effect of gain saturation on the radial distribution of modes u_{00}^{HG} (a, b) and u_{10}^{HG} (c, d) in the near-field (a, c) and far-field (b, d) domains for $Q_{in}^{max} = 0.1Q_s$ and the small-signal gain $G_0 = 4$ and 16; the dashed curves are the distributions for input beams.

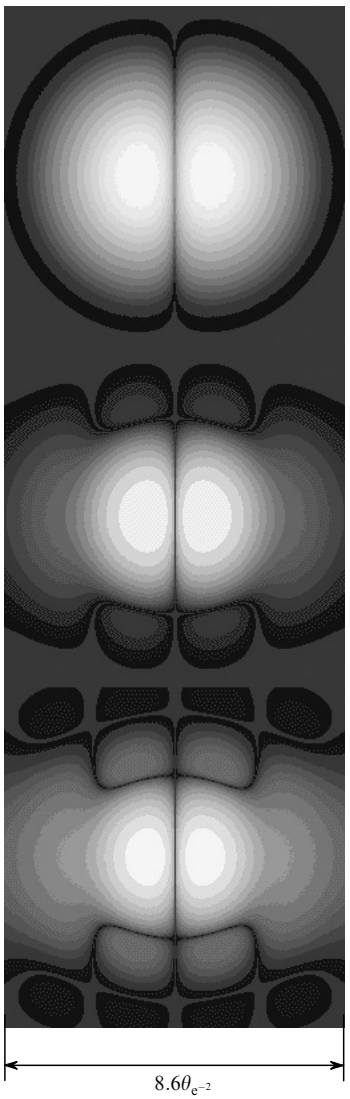

Figure 2. Two-dimensional far-field distribution patterns of the u_{10}^{HG} mode (logarithmic scale) for the initial beam for the energy density in the maximum $0.1Q_s$ (a) and for saturated gain for $G_0 = 4$ (b) and 16 (c).

where $G_{nf}(u_{mn}^{HG})$ is the near-field distribution of the amplitude of the mode u_{mn}^{HG} after amplification. The results of expansions for the modes u_{00}^{HG} and u_{10}^{HG} ($G_0 = 16$) are presented in Fig. 3 and can be written in the form

$$G_{nf}(u_{00}^{HG}) \sim \sum_{j=0}^{\infty}\sum_{k=0}^{\infty} a_{2j,2k}^{nf} u_{2j,2k}^{HG}, \tag{3}$$

$$G_{nf}(u_{10}^{HG}) \sim \sum_{j=0}^{\infty}\sum_{k=0}^{\infty} a_{2j+1,2k}^{nf} u_{2j+1,2k}^{HG}, \tag{4}$$

where $a_{2j,2k}^{nf}$ and $a_{2j+1,2k}^{nf}$ are the amplitude expansion coefficients, which are real numbers for the model of an infinitely thin amplifier used here. A similar expansion in the far-field domain is simply the Fourier transform (FT) of expressions (3) and (4) and, for example, for the u_{10}^{HG} mode this gives the complex expansion coefficients

$$a_{2j+1,2k}^{ff} = a_{2j+1,2k}^{nf} \exp[-i\pi(k + j + \tfrac{1}{2})]. \tag{5}$$

According to Figs 3a, b, upon gain saturation ($G_0 = 16$), no more than $\sim$0.4 % of the total energy fall within the high-

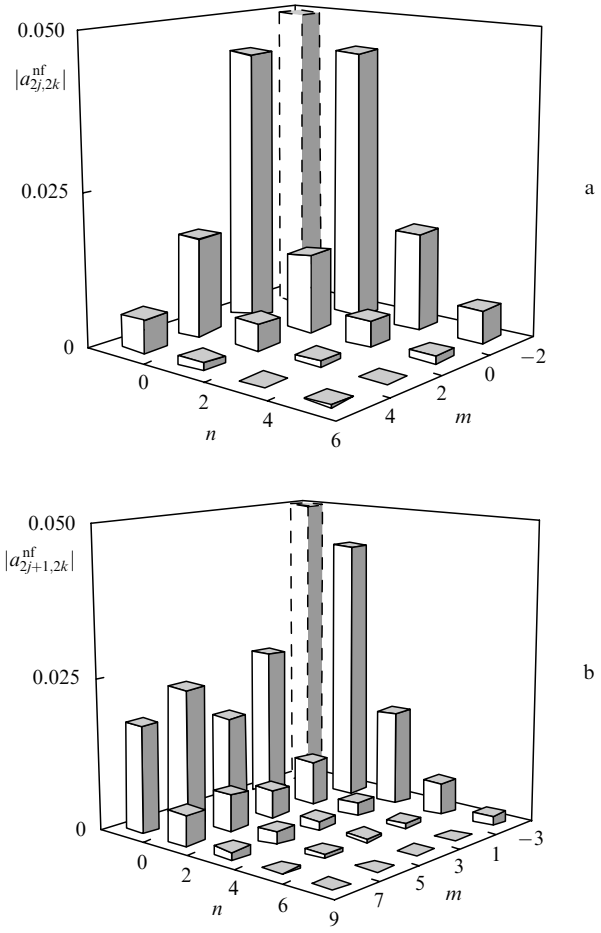

Figure 3. Modal radiation spectrum for the u_{00}^{HG} (a) and u_{10}^{HG} modes (b) amplified with saturation ($G_0 = 16$). The moduli of the weight coefficients of the fundamental modes in the spectrum (shown by the dashed straight lines) are presented not in the scale.

order modes (for $G_0 = 128$, calculations give $\sim$4.2 %). However, this proves to be quite sufficient for the appearance of phase dislocations in the laser beam, whose view for the u_{10}^{HG} mode is shown in Figs 2b, c.

2.2 Conversion of the Hermite – Gaussian modes to Laguerre – Gaussian modes in the presence of distortions caused by gain saturation

The gain saturation leading to a considerable enrichment of the modal spectrum of laser radiation cannot fail to affect the result of conversion of the HG modes to LG modes by means of an astigmatic $\pi/2$-converter [14] or by some other method [15, 16].

As for astigmatic $\pi/2$-converters, they can use FTs both of the integer and fractional (including irrational) orders* [17]. In this case, the u_{mn}^{HG} mode at the input to the $\pi/2$ converter in the coordinate system coupled with the orientation of cylindrical lenses is a sum of the $u_{m'n'}^{HG}$ modes

* The fractional FT is defined by the expression

$$\mathscr{F}_x^b[f(x)] = \frac{\exp(i\psi/2)}{\sqrt{i\sin\psi}} \int_{-\infty}^{+\infty} f(\xi) \exp\left[i\pi \frac{(x^2 + \xi^2)\cos\psi - 2\xi x}{\sin\psi}\right] d\xi,$$

where $b = 2\psi/\pi$ is the FT order ($b = 1$ gives the usual FT). The scheme of an astigmatic $\pi/2$-mode converter includes a set of cylindrical (or cylindrical and spherical) lenses performing FTs in mutually orthogonal planes, whose orders differ by unity.

of the same order ($m+n=m'+n'$) in a new basis, each of them acquiring the phase shift

$$\mathscr{F}_{x'}^{a}\{\mathscr{F}_{y'}^{a+1}[u_{m'n'}^{\mathrm{HG}}(x',y')]\}$$

$$=\exp\{-\mathrm{i}\pi[a(m'+n')+n']/2\}u_{m'n'}^{\mathrm{HG}}(x',y'), \qquad (6)$$

where $\mathscr{F}_{\xi}^{b}$ is the operator of the FT of the order b in coordinate ξ. Therefore, the intensity and phase distributions at the converter output depend not only on the order of the HG mode of the initial radiation, maximum energy density, and gain, but also on the order of FTs used in a $\pi/2$-converter.

Consider first the results of calculations for a $\pi/2$-converter of the order $a=0.5$ (the scheme of this converter is presented in Fig. 2 in [18]). Figures 4a–e show the dependences of the intensity and phase distributions and phase dislocations on the gain for a fixed maximum energy density $Q_{\mathrm{in}}^{\max}=0.1Q_{\mathrm{s}}$ for the u_{10}^{HG} mode (phase distributions are presented on a linear grey $0-2\pi$ scale). Note that all screw dislocations in Figs 4d, e have the same sign of the topological charge. However, the addition of nonlinear absorption to the saturated gain, which is described by the expression having the physical sense close to (1), gives additional screw dislocations with the opposite sign (indicated by the arrow in Fig. 4f).

Another effect of the gain saturation, which can be more substantial in some applications than the production of phase dislocations, is the distortion of the energy density (intensity) distribution in the circular distribution of LG modes. Thus, for the u_{01}^{LG} mode (Figs 4a, b) for $G_0=16$, we have $Q_{\mathrm{out}}^{\max}(r_{\max})/Q_{\mathrm{out}}^{\min}(r_{\max})=1.2$. Recall that the admixture of higher modes in this case is only 0.4 % of the total beam energy at the $\pi/2$-converter input.

The gain saturation for HG modes accompanied by their conversion to LG modes not only gives rise to new phase dislocations (mainly at the beam periphery) but also results in the decay of screw phase dislocations typical for the u_{0l}^{LG} modes. This is demonstrated by the results of calculations for the u_{03}^{LG} mode presented in Fig. 5, where the near-axis regions of the phase distribution are given on an enlarged scale in Figs 5e, f. Here, all the three elementary screw dislocations are located on the y axis (the initial u_{30}^{HG} mode is oriented along the x axis) and the distance between them increases with increasing G_0. Note that a greater size of the beam region around a singularity with an uncertain phase in Fig. 5e ($G_0=4$) reflects the physical reality, namely, the smaller value of $\mathrm{d}Q/\mathrm{d}r$ than in Fig. 5f ($G_0=16$). The size of the region with an uncertain phase in these figures is determined by the cut-off level of the field amplitude ($\sim 10^{-3}$ of the maximum) below which the FRESNEL program cannot map the reconstructed phase.

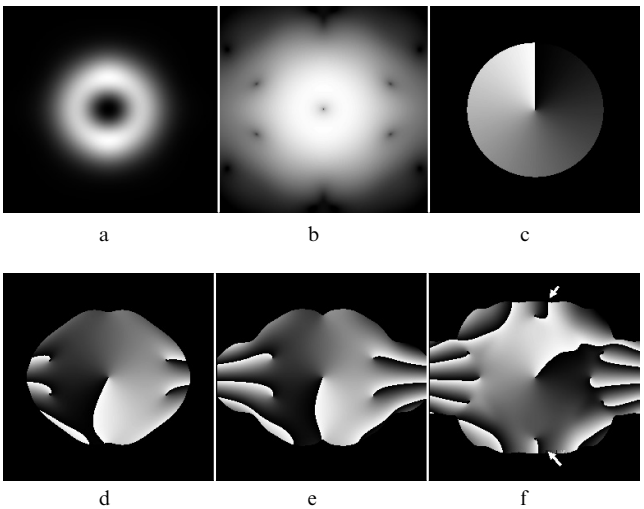

Figure 4. Conversion of the u_{10}^{HG} mode to the u_{01}^{LG} mode upon gain saturation. The intensity distributions ($G_0=16$) on the linear (a) and logarithmic (b) scales and phase distributions upon amplification without saturation (c), with saturation for $G_0=4$ (d) and 16 (e), and gain and absorption saturation (f).

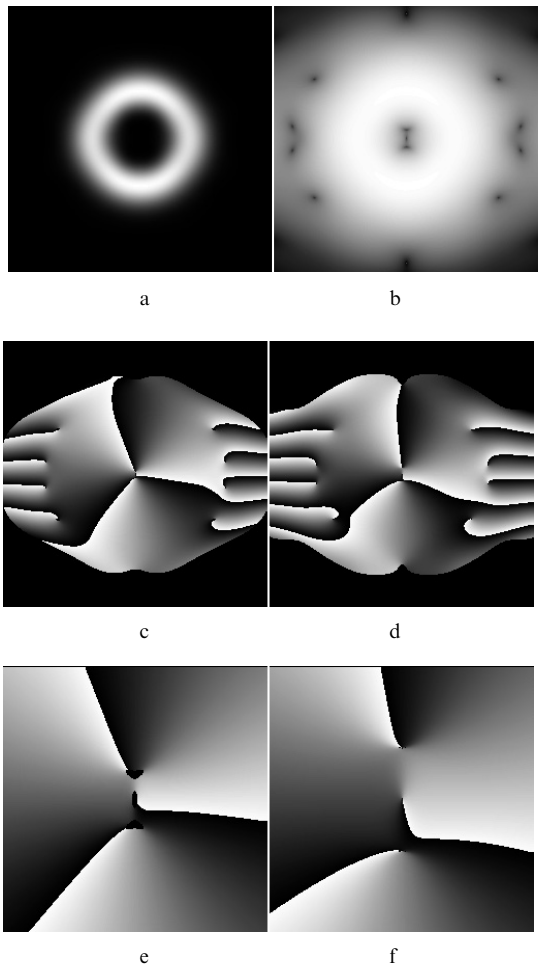

Figure 5. Conversion of the u_{30}^{HG} mode to the u_{03}^{LG} mode in the case of gain saturation. The intensity distributions ($G_0=16$) on the linear (a) and logarithmic (b) scales and phase distributions for $G_0=4$ (c) and 16 (d); e and f are the axial regions of distributions c and d, respectively.

As follows from the calculation (Fig. 6), upon gain saturation in the chosen scheme of an astigmatic $\pi/2$ converter, the location of elementary singularities formed in the near-axis region of the corresponding LG modes obeys a rather simple rule: for the initial u_{m0}^{HG} mode ($m>1$), we have $m-2$ singularities of a unit topological charge on the x axis and two similar singularities on the y axis. This rule, however, should be somewhat reformulated when a different scheme of the converter is used. Thus, Figure 7

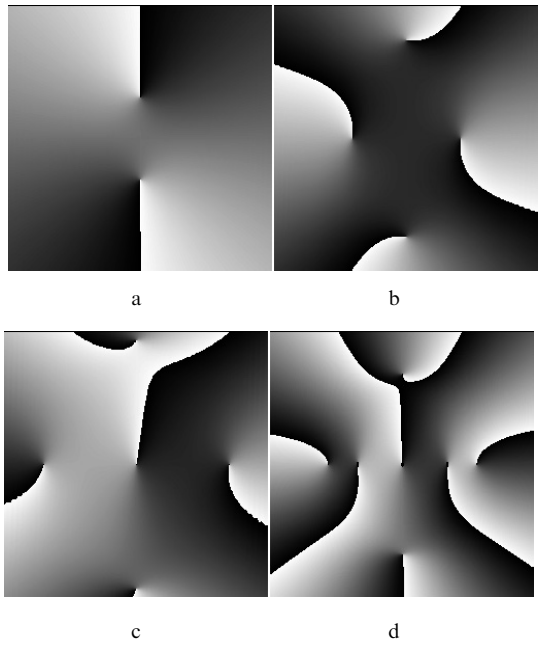

Figure 6. Location of the near-axis phase singularities of LG modes obtained after amplification with the saturation of the u_{m0}^{HG} modes for $m = 2$ (a), 4 (b), 5 (c), and 6 (d).

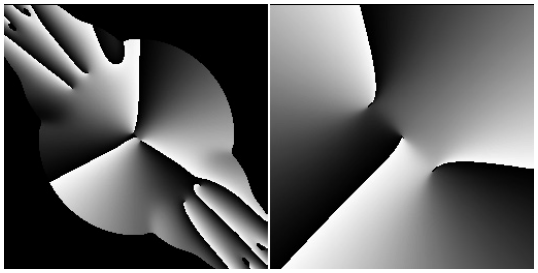

Figure 7. Change in the phase distribution for the u_{03}^{LG} mode for an astigmatic $\pi/2$-converter with the integer Fourier transforms (see text).

shows the calculation for the u_{30}^{HG} mode and a converter based on the scheme from [14], in which the Fourier-transform order is $a = 1$. Here, the gain, energy density at the maximum and the location of the HG mode ($m = 3$ along the x axis) are the same as in Figs 5d, f. In other words, the modal spectrum of the beam at the converter input was not changed. In this case, both the location of near-axis singularities and the structure of singularities at the beam periphery somewhat differ from those for a converter with $a = 0.5$, which can be explained taking into account a change in the phase shift of the modes according to (6).

Finally, note that the gain saturation for the HG mode accompanied by its conversion to the LG mode results in a change in the orbital angular momentum J of the beam [19] at the $\pi/2$-converter output. In our case, the z component of the orbital angular momentum is

$$J_z = \frac{\int_{-\infty}^{+\infty}\int_{-\infty}^{+\infty} Q(x,y)\left(y\frac{\partial \Phi}{\partial x} - x\frac{\partial \Phi}{\partial y}\right)\mathrm{d}x\mathrm{d}y}{\int_{-\infty}^{+\infty}\int_{-\infty}^{+\infty} Q(x,y)\mathrm{d}x\mathrm{d}y}, \qquad (7)$$

where $\Phi = \Phi(x, y)$ is the phase distribution in the beam (in radians) and J_z is expressed in $\hbar$ (Plank's constant) per photon. In particular, the spectrum of the u_{10}^{HG} beam after amplification (see Fig. 3b) includes the HG modes, which can be transformed to the LG modes both with the same ($m > n$) and opposite ($m < n$) sign of the screw dislocation. The total energy [a sum of squares of weight coefficients (2)] of these two groups of modes is approximately the same and amounts to $\sim 0.2\,\%$ of the total energy for $G_0 = 16$ (for a sum of all the modes of the expansion up to $u_{11,10}^{HG}$, the calculations give 99.986 %). As a result, the calculations for a beam with distributions $Q(x, y)$ and $\Phi(x, y)$ presented in Figs 4a, b, e, give $J_z = 0.957$ instead of $J_z = 1$ for the unperturbed u_{01}^{LG} mode.

2.3 Phase distortions of the Laguerre–Gaussian modes upon gain saturation

The results of calculations presented above show that in the case of gain saturation, a variation in the spatial distribution of the energy density in the u_{m0}^{HG} beams mainly affects the structure of phase dislocations upon the HG–LG mode conversion.

The phase distortions of the LG modes can be weakened (it is unlikely that they can be completely avoided because the generation of the initial HG modes in lasers is related to

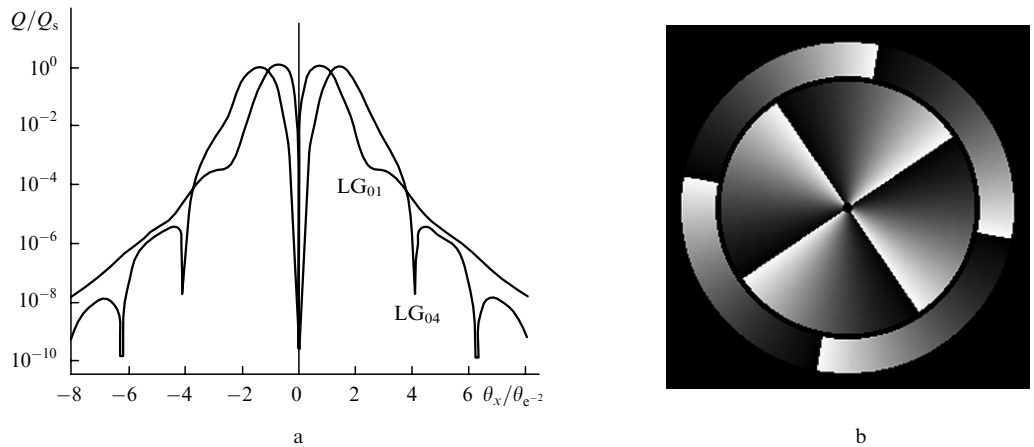

Figure 8. Intensity (a) and phase (b) distributions upon gain saturation for the u_{01}^{LG} и u_{04}^{LG} modes (a) and the u_{04}^{LG} mode (b).

a some degree with a decrease in the inversion in the active medium) if the amplification and conversion of HG modes are interchanged. In this case, the gain saturation should result (in the ideal case) in the production of edge dislocations in the far-field domain, which is confirmed by our calculations (Fig. 8) performed, as above, for $Q_{\text{in}}^{\max} = 0.1Q_s$. The type of edge phase dislocations (Fig. 8b), except the phase term $\sim\exp(-il\varphi)$, is completely similar to the type of dislocation for the u_{00}^{HG} mode in section 2 (Fig. 1). Note that the edge phase dislocations for the u_{01}^{LG} mode (Fig. 8a) are not manifested at any G_0. This is similar to their absence (on the x axis) for the u_{10}^{HG} mode (Fig. 1d), which is explained by the decay law $\sim r^2\exp(-r^2/w_0^2)$ for $Q(x,y)$ at the beam periphery, which differs from the dependence of the energy density on r for modes of other types.

Due to the symmetry of LG beams, the gain saturation results in a weak enrichment of the modal spectrum and no variations in the orbital angular momentum occur. For example, the spectrum of the u_{04}^{LG} beam (Fig. 8) includes predominantly the u_{p4}^{LG} modes with the topological charge $l = 4$. In this case, 99.997 % of the total energy is contained in the first six modes ($p = 0 - 5$).

3. Conclusions

As follows from the expansion of the amplified beams in the basis of HG modes, a change in the number and character of phase dislocations in the far-field domain with increasing G_0 is directly caused by the gain saturation, resulting in the enrichment of the modal spectrum of radiation, and by an increase in the relative weight of higher-order modes. The gain saturation described by the relation similar to the Frantz–Nodvik equation gives, of course, the same result. Similar effects should be also observed upon multiphoton absorption. The only difference is that the gain (absorption) saturation for pulsed laser fields is manifested to a greater degree by the pulse end, where $Q(t)$ achieves its maximum. Upon multiphoton absorption, however, the appearance of phase dislocations is related to the maximum pulse intensity $I(t)$. In both cases, the production and decay of phase dislocations is a dynamic process. In turn, the time-dependent phase variations in laser beams should give rise to spectral singularities localised near the singularity points and lines.

Phase dislocations also take place in the stationary case upon the coherent mixing of many modes or, for example, if the spatial distribution of linear absorption or the refractive index causes the deformations of the intensity (energy density) distribution similar to these described in the paper. In this case, the creation and decay of phase dislocations develops in space during the propagation of radiation from the near- to far-field domain or vice versa.

From the practical point of view, it is important that the quality of high-power LG beams is significantly improved if the HG–LG mode conversion by means of astigmatic $\pi/2$ converters is performed before their amplification.

Acknowledgements. This work was supported by the Russian Foundation for Basic Research (Grant No. 05-02-16818).

References

1. Bandres M.A., Gutierrez-Vega J.C. *Opt. Lett.*, **29**, 144 (2004).
2. Kimel I., Elias L.R. *IEEE J. Quantum Electron.*, **29**, 2562 (1993).
3. Tovar A.A., Casperson L.W. *J. Opt. Soc. Am. A*, **15**, 2425 (1998).
4. Tovar A.A. *J. Opt. Soc. Am. A*, **17**, 2010 (2000).
5. Mamaev A.V., Saffman M., Zozulya A.A. *Phys. Rev. Lett.*, **77**, 4544 (1996).
6. Abramochkin E.G., Volostnikov V.G. *Usp. Fiz. Nauk*, **174**, 1273 (2004).
7. Velchev I., Dreischuh A., Neshev D., Dinev S. *Opt. Commun.*, **140**, 77 (1997).
8. Motzek K., Kaiser F., Salgueiro J.R., Kivshar Y., Denz C. *Opt. Lett.*, **29**, 2285 (2004).
9. Petrov D.V. *Opt. Commun.*, **200**, 381 (2001).
10. Petrov D.V. *Opt. Commun.*, **188**, 307 (2001).
11. Kreminskaya L.V., Soskin M.S., Khizhnyak A.I. *Opt. Commun.*, **145**, 377 (1998).
12. Frantz L.M., Nodvik J.S. *J. Appl. Phys.*, **34**, 2346 (1963).
13. www.wavesumsoft.com.
14. Beijersbergen M.W., Allen L., van der Veen H.E.L.O., Woerdman J.P. *Opt. Commun.*, **96**, 123 (1993).
15. Bazhenov V.Yu., Vasnetsov M.V., Soskin M.S. *Pis'ma Zh. Eksp. Teor. Fiz.*, **52**, 1037 (1990).
16. Beijersbergen M.W., Coerwinkel R.P.C., Kristensen M., Woerdman J.P. *Opt. Commun.*, **112**, 321 (1994).
17. Malyutin A.A. *Kvantovaya Elektron.*, **34**, 165 (2004) [*Quantum Electron.*, **34**, 165 (2004)].
18. Malyutin A.A. *Kvantovaya Elektron.*, **35**, 76 (2005) [*Quantum Electron.*, **35**, 76 (2005)].
19. Allen L., Beijersbergen M.W., Spreeuw R.J.C., Woerdman J.P. *Phys. Rev. A*, **45**, 8185 (1992).